



## Review

# Homotropic and heterotropic interactions in cytochromes $c_3$ from sulphate reducing bacteria

David L. Turner<sup>a,\*</sup>, Teresa Catarino<sup>a,b</sup><sup>a</sup> Instituto de Tecnologia Química e Biológica, Universidade Nova de Lisboa, Av. da República, 2780-157 Oeiras, Portugal<sup>b</sup> Departamento de Química, Faculdade de Ciências e Tecnologia, FCT, Universidade Nova de Lisboa, 2829-516 Caparica, Portugal

## ARTICLE INFO

## Article history:

Received 30 May 2011

Accepted 4 July 2011

Available online 14 July 2011

Edited by Miguel Teixeira and Ricardo O. Louro

This article is dedicated to the memory of António Xavier

## Keywords:

Cytochrome  $c_3$   
Multihaem protein  
Cooperativity  
Electron transfer  
NMR

## ABSTRACT

**This article reviews the contribution of António Xavier and his associates to the study of multihaem cytochromes. Detailed analysis of interactions between the charges of the haems and protonatable groups reveals that electrostatic effects may be outweighed by subtle changes in conformation. This helps us to understand how tetrahaem cytochromes  $c_3$  work and also gives an insight into the mechanism of cytochrome  $c$  oxidase.**

© 2011 Federation of European Biochemical Societies. Published by Elsevier B.V.

Open access under [CC BY-NC-ND license](http://creativecommons.org/licenses/by-nc-nd/3.0/).

## 1. Introduction

Although our task is to summarise our recent work on electron–proton coupling in multihaem cytochromes, this cannot be separated from the work of António Xavier, with whom we had a long and fruitful collaboration. However, this discussion addresses only a fraction of his work since our involvement in it is distinctly biophysical. A more biological discussion can be found in the review by Louro [1]. Detailed and comprehensive studies such as those outlined in this review have been largely, though not exclusively, confined to our group and those of former Ph.D. students of António Xavier. The review would serve a purpose if it brings the techniques for characterisation of multicentre proteins to a wider audience.

The properties of the tetrahaem cytochromes  $c_3$  from sulphate reducing bacteria are the subject of most of the work, together with the development of the methodology needed to explore them and the insights that have been gained. A typical cytochrome  $c_3$  is shown in Fig. 1; it contains four haems  $c$ , each with two histidine ligands, and barely enough polypeptide to hold them together.

The amino acid sequences of the various proteins that have been characterised to date show little homology beyond the haem binding sites and yet the geometry of the haems is highly conserved. This suggests that it is of vital importance to control the rates of intramolecular electron transfer (ET). Unfortunately, unlike the variety of centres found in photosystems, the close similarity between the haems has not yet allowed us to pursue the matter of intramolecular ET further than the original observation that it is “fast”. Indeed, the only method capable of clearly discriminating between the four haems is NMR. That brought cytochromes  $c_3$  to the attention of Bob Williams’ group [3] and so to the attention of António Xavier.

Much of our work with cytochromes  $c_3$  has been directed towards comparative studies of the structures and thermodynamic properties of the proteins from a variety of organisms. It was established early on that the redox potentials of the haems are pH dependent, i.e., there is an energy of interaction between electrons and protons. Some interaction is an inevitable consequence of electrostatics, but it also makes sense because cytochrome  $c_3$  is a partner for a [NiFe] hydrogenase and so is a prime candidate for transporting the two electrons and two protons released by splitting hydrogen. Since our studies showed that the interactions are not simply electrostatic, the effect of protonation on the structure becomes of interest and NMR is once again the best technique, this

\* Corresponding author. Fax: +351 21 4411277.

E-mail address: [turner@itqb.unl.pt](mailto:turner@itqb.unl.pt) (D.L. Turner).

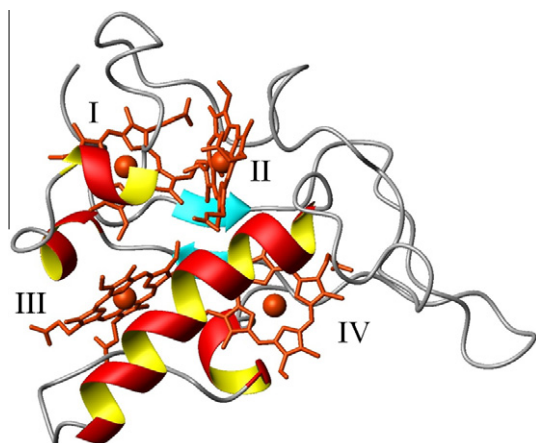


**Fig. 1.** X-ray structure of the tetrahaem cytochrome  $c_3$  from *Dsm. baculatum* [2]. The haems are numbered according to the positions of their binding sites in the aminoacid sequence.

time for determining structures with full control over the solution potential and pH. It is not sufficient to study the cytochrome in isolation, but its natural partners – the [NiFe] hydrogenase on the one hand and a membrane protein complex on the other – are difficult to study. One of our current projects may offer a way around this, and it will be discussed as further work.

## 2. Thermodynamic properties of cytochromes $c_3$

Both EPR and NMR were used to demonstrate that the redox potentials of cytochromes  $c_3$  are pH dependent [4,5]. There were limitations to these studies because, although there are small

differences between the  $g$ -values of the four haems and more substantial differences in the chemical shifts of the haem protons, the signals were not assigned to individual haems. That is now much easier, with three-dimensional structures to give some clue to the expected  $g$ -values and two-dimensional NMR to assist in obtaining total assignments of protein spectra. However, the biggest problem lies in the complexity of the system. Each of the four haems can be found in two states, with FeII or FeIII, and the pH-dependent redox potentials involve protonatable groups. Only one of the cytochromes  $c_3$  examined to date shows the clear effect of two separate protonations [6], so it is usually sufficient to consider a single protonatable group which can, of course, exist in two states. Thus, we should consider 32 different forms (we call these microstates; see Fig. 2). In principle, we would like to characterise each of the microstates but that is not practical.

Instead of treating the energy of each microstate as a separate parameter, it is convenient to consider energy differences. For example, each haem has a redox potential which represents the energy difference between two microstates, and this redox potential may change with changes in the oxidation state of neighbouring haems or the protonatable centre. The 32 energies can then be represented as sums of four redox energies in some reference state, the deprotonation energy for the ionisable group, and interaction terms that depend on the state of the five different centres. There are still 32 parameters and they cannot all be determined experimentally. There are 10 such terms for pairwise interactions, 10 more for groups of three centres, 5 for groups of four, and 1 for all five. If only pairwise interactions are considered and the higher order interactions are neglected then we are left with only 15 parameters (strictly 16 if we include a reference value), which is at the limit of what can be determined. This is the model that we have used; it requires only four values of  $e_0$ , six haem–haem interactions, one  $pK_a$ , and four interactions between the proton and the haems [7].

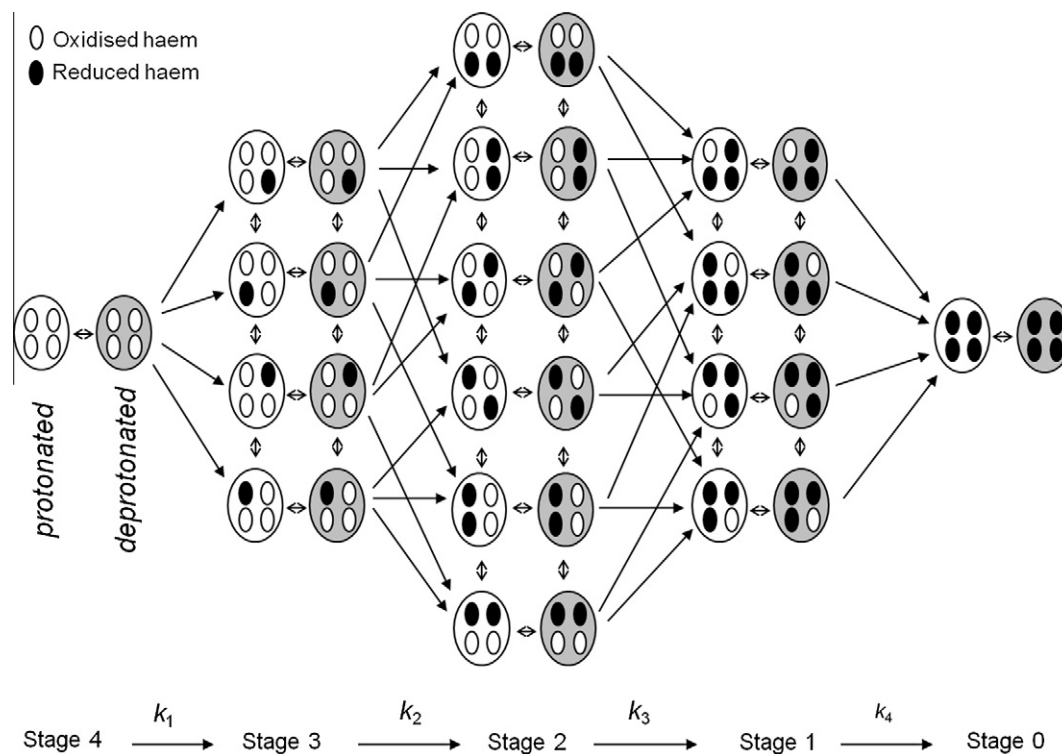


**Fig. 2.** Schematic representation of the microstates of a cytochrome with four haems and one protonatable group. Double-headed arrows indicate fast intramolecular electron exchange and proton exchange with the solvent; at least one protonation site is necessary to fit experimental data. Single-headed arrows indicate individual electron transfer steps: weighted averages of these microsteps give the observable reduction rate constants  $k_1$ – $k_4$ .

Most measurements yield information in the form of concentrations or populations, which are readily related to the 15 parameters via the energies of the microstates. If the haems are numbered 1–4 and the protonatable group is number 5 then the energies have a very simple form:

$$g_m = \sum_{i=1}^{i=5} g_i + \sum_{i=1, j=i+1}^{i,j=5} g_{ij} \quad (1)$$

where the terms  $g_i$  are zero unless the centre  $i$  is oxidised or deprotonated, and the terms  $g_{ij}$  are zero unless both centres  $i$  and  $j$  are oxidised or deprotonated. In normal practice, the redox energy is quoted in volts and the deprotonation energy is referred to as a  $pK_a$ , so the equation requires some constants to be strictly correct:

$$G_m = \sum_{i=1}^{i=4} F(e_{0i} - E_s) + 2.3RT(pK_a - pH) + \sum_{i=1, j=i+1}^{i,j=5} g_{ij} \quad (2)$$

with terms being zeroed as above:  $F$  is the Faraday constant,  $e_{0i}$  is the reduction potential of haem  $i$  in stage zero, and  $E_s$  is the solution potential.

It is important to note that the protein conformational energy may change from microstate to microstate but it would be absorbed into the apparent redox potentials or the  $pK_a$ . The price paid for neglecting higher order interactions is that, if it were possible to measure them, different values for the pairwise interactions might be obtained from studies of largely oxidised or largely reduced samples. Similarly, neglecting the interactions with the protonation site would mean that the remaining parameters appear to vary with pH. Hence any further simplification in the model is likely to render the parameters uninformative.

In practice, measurements are made by a combination of NMR and redox titrations monitored by UV–Vis spectroscopy. The redox titrations monitor the total oxidised haem as a function of solution potential: the position of the curve gives absolute redox potentials and its shape calibrates the interactions. This information could also be obtained by NMR but for the difficulty of measuring potentials in 5 mm NMR tubes and the relatively low accuracy with which signal intensities can be measured. The NMR experiments measure the paramagnetic shifts of methyl substituents of the haems. Under typical conditions, intramolecular electron exchange is fast on the NMR timescale, whereas intermolecular exchange is slow. This means that the signal of a haem methyl in a particular stage is a weighted average over the microstates and the resulting paramagnetic shift is a measure of the average fraction of oxidation of each haem. Proton exchange is moderately fast, so averaged shifts are obtained, though some line broadening is observed [7]. Intermolecular exchange is usually slow enough to give separate signals for each stage but fast enough to generate cross-peaks in two-dimensional exchange experiments. That makes it possible to assign all of the signals of an intermediate stage by making the assignments in the fully oxidised or reduced forms, preferably both, and following the peaks through the different stages using 2D spectra of partially reduced samples, as illustrated in Fig. 3. Although it is more convenient to assign the NMR signals of the haems with respect to the structure, it is not necessary to do so: the thermodynamic model does not use any structural information and it is sufficient to find signals from four different haems. In the unrelated tetrahaem domains of fumarate reductases from *Shewanella* spp., this approach immediately confirmed the assignments of haems II

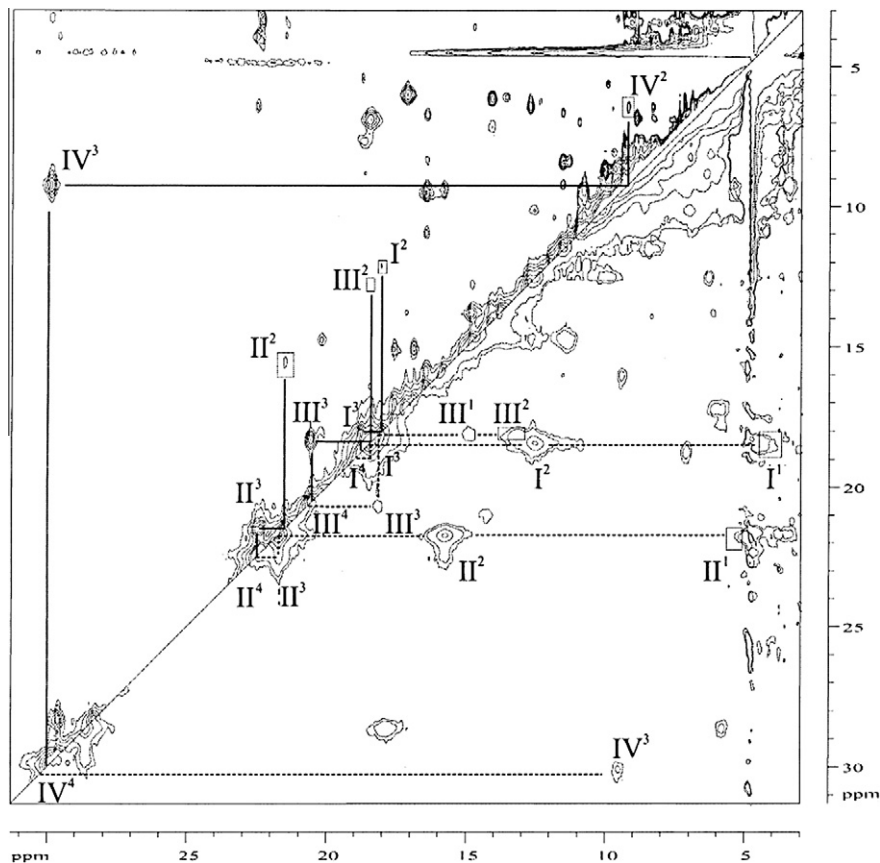


**Fig. 3.** Two-dimensional NMR exchange spectra of partially oxidised cytochrome  $c_3$  from *D. vulgaris* Hildenborough (from [9]). The lines connect signals of particular methyl groups (Roman numerals) in different oxidation stages (Arabic superscripts) to exchange cross-peaks. The sample used for the spectrum above the diagonal was more oxidised than that below.

and III because of their close proximity and the large interaction between them [8].

Cytochromes  $c_3$  from several different sulphate reducing bacteria have been analysed using this thermodynamic model and there is surprisingly little similarity between them [2,10,11]. It might seem advantageous to have a haem that is largely oxidised as the initial electron acceptor, and one that is largely reduced as the donor. However, any one of the haems may be first to oxidise, though it is usually I or II, and the last haem to oxidise is usually III or IV. In fact it is only necessary that the accepting haem is partially oxidised, and that the donating haem is partially reduced, because intramolecular transfer is fast.

Several cytochromes  $c_3$  have a cluster of lysines close to haem IV [1], this 'lysine patch' has been proposed to be a docking site for hydrogenase, the electron donor. Work with the cytochrome  $c_3$  and [NiFe] hydrogenase from *Desulfovibrio vulgaris* Miyazaki F indicated an interaction in the region of haem IV and studies of electron transfer kinetics showed that mutants in which Lys was replaced by Met close to haem IV had higher apparent  $K_m$  values [12]. In the type I cytochrome  $c_3$  from *Desulfovibrio africanus*, a possible docking site for the electron acceptor, type II cytochrome  $c_3$ , was identified near haem III, which is the last to oxidise in that case, and another near to haem IV [13]. In fact it would be convenient to have haem IV of cytochrome  $c_3$  as the contact point both with the donor hydrogenase and with the acceptor at the membrane since this would discourage the formation of ternary complexes. However, there is no consistency in the position of haem IV in the order of oxidation (see Table 1).

The picture of protonation is not much clearer, with the strongest electron–proton interaction (frequently called a redox–Bohr interaction) often being with haem I, which suggests that the ionisable group may be a propionate of haem I [14]. But haem III has the strongest redox–Bohr interaction in the proteins from *Desulfovibrio norvegicum* and *Desulfovibrio baculatum* [2]. Modelling the data for the protein from *Desulfovibrio desulfuricans* requires two protonatable groups: the strongest interaction is for haem I and the second proton affects haems II and III. This variety of interactions is not so surprising in view of local variations in the protein dielectric constant and changes in conformation. The haem–haem interactions highlight the point: most cytochromes  $c_3$  have one interaction that is small or even negative, i.e., reducing one haem favours the reduction of a second one, in direct opposition to the expected Coulombic interaction between two negative charges (see, for example, Fig. 4 and the interactions of cytochrome  $c_3$  from *D. vulgaris* Hildenborough in Table 2). This is intriguing in view of the expectation that cytochromes  $c_3$  transport pairs of electrons. These positive cooperativities must involve some change in conformation such as the movement of charged groups in the vicinity of the interacting haems so that the electrostatic interaction with the haem charge is cancelled. In other words, the effective

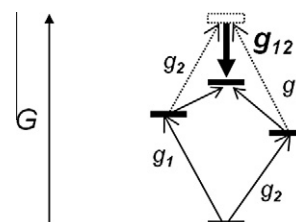


**Fig. 4.** Energy diagram for two centres with positive cooperativity. Note that a change in state of centre 1 makes it easier to change centre 2 (and vice versa) because of the negative interaction energy,  $g_{12}$ .

**Table 2**

Thermodynamic parameters for cytochrome  $c_3$  from *D. vulgaris* Hildenborough. Energies are given in meV with respect to the fully reduced and protonated protein. The diagonal terms in bold are the energies for each centre and the terms above the diagonal are interaction energies (the conversion factor from pH units to Volt is  $2.3RT/F$ ). The interactions between the haems and the protonatable centre are all of negative sign, which represents a positive cooperativity as expected between electrons and protons. The interaction energy between haem I and haem II is also negative, which cannot be explained by electrostatics alone.

	Haem I	Haem II	Haem III	Haem IV	Protonatable centre
Haem I	<b>−252</b> (2)	−39 (1)	19 (1)	3 (3)	−74 (3)
Haem I		<b>−284</b> (2)	1 (1)	10 (2)	−36 (2)
Haem I			<b>−343</b> (1)	34 (2)	−23 (2)
Haem I				<b>−293</b> (2)	−14 (2)
Protonatable centre					<b>+454</b> (3)

interaction between two charges in a protein may have the opposite sign to that predicted by electrostatics because the conformational energy of the protein has to be taken into account.

### 3. Kinetic properties of cytochromes $c_3$

All cytochromes  $c_3$  show electron self-exchange, which is the key to the thermodynamic studies outlined in the previous section, but that is obviously non-physiological. The self-exchange rates are higher in a few cytochromes with more exposed haems or lower charge, making it necessary to use lower concentrations, lower temperatures, or high ionic strength to achieve slow exchange on the NMR timescale. At near-neutral pH, the exchange of the proton responsible for the redox–Bohr interaction may also be observable [7]. This is because the change in the relative haem redox potentials alters the balance of populations of microstates within each redox stage and so changes the paramagnetic shifts of the haem methyl protons. The signals are not split because they are nearly in fast exchange, but they may exhibit broadening. Analysis shows that the proton exchange rate is diffusion limited, which might be expected for a proton that is taken up during the lifetime of an encounter complex.

Probing the kinetics of reduction of these multihaem cytochromes in detail is even more difficult than the thermodynamic analysis. All of the haems have some surface exposure and react rapidly with reductants such as  $\text{SO}_3^{2-}$  from dithionite. Once an electron has been transferred, it equilibrates rapidly among the haems so that there is no trace of its starting point. Thus, in stepping from stage to stage, electrons may be injected through any haem. There will also be a mixture of redox stages present during the reduction. Stopped flow experiments with UV–Vis detection are a convenient method to follow these fast reactions but that only gives the total reduced haem across the whole sample: even if the four consecutive reduction steps have distinct rates (with contributions from

**Table 1**

Order of oxidation of the haems in various cytochromes  $c_3$ . These orders apply in the protonated forms: large redox–Bohr effects may change the order at higher pH. The haems (numbered in order of their binding sites in the aminoacid sequence) with the highest redox–Bohr interaction energies are shown in bold.

Source	Haem order
<i>D. gigas</i>	<b>I</b> , II, III, IV
<i>D. vulgaris</i> Hildenborough	III, IV, <b>II</b> , <b>I</b>
<i>D. vulgaris</i> Miyazaki F	III, II, IV, <b>I</b>
<i>D. desulfuricans</i> ATCC27774	II, <b>I</b> , III, IV
<i>Dsm. norvegicum</i>	II, I/IV, <b>III</b>
<i>Dsm. baculatum</i>	II, I/IV, <b>III</b>
<i>D. africanus</i> (type I)	<b>I</b> /IV, II, III
<i>D. africanus</i> (type II)	<b>II</b> /III, I, IV

each of the haems), each trace will yield a maximum of four composite rate constants (see Fig. 2).

It has proved possible to extract kinetic data for the individual haems using thermodynamic data and some fairly reasonable assumptions [15]. The rate of reduction of a haem depends on the fraction of the time that it spends oxidised: these fractions are available for each of the oxidation stages. We assume that the process is collisional, i.e., the electron transfer (ET) step is rate determining with fast equilibration of the protein, reducing agent, and ET complex. Next we assume that the electron transfer rate depends on the driving force according to Marcus theory and that the reorganization energy is similar for all haems. The driving force for the reduction of any microstate is available from a thermodynamic analysis.

It should be mentioned that a major component of the changes in driving force is electrostatic, and charge–charge interactions between the protein and reducing agent might also be significant. However, the major concentration of charge is at the haem irons, which are buried, and a surface charge that might change close to one haem is necessarily far from the others. Our attempts to simulate the effective rates of reduction with Monte Carlo calculations with electrostatic interactions failed to reproduce even broad trends, so the neglect of interactions with surface charges seems reasonable.

Finally, we must make an assumption in order to reduce the number of parameters to four, which is the number of observable rate constants. Two possibilities provide a useful internal check. We may assume that each haem has an intrinsic rate (its reference rate) that is modified by changes in population and driving force but that there is no change in any other factor, such as surface exposure, that might change the rates between stages. This will al-

low the data to be analysed in terms of the four reference rates. Alternatively, we may assume that significant changes do occur between stages, but then we are forced to assume that the intrinsic rates for the haems are all the same and they share a reference rate which is different for each electron transfer step. That also yields a model with four variables.

In practice, these models describe the experimental results well enough for the kinetic data to be fitted simultaneously with the thermodynamic results (paramagnetic shifts and redox titrations). Further, if there is any significant difference in the quality of fit with the two possible models, then the model that assumes that the variation among haems is more important than the differences between the redox stages is the winner.

Perhaps unsurprisingly, the reference rate constants of the individual haems are almost as varied as their orders of oxidation (Table 3). There is no simple correlation of the intrinsic rates with the exposure of the haem to the solvent or with surface charges. The lysines close to the exposed part of haem IV might be expected to attract  $\text{SO}_2^-$  but the rates obtained for haem IV are unremarkable. Of course, the  $\text{SO}_2^-$  radical is nothing like the proteins that are physiological partners. Nevertheless, these studies have given us even greater confidence in the thermodynamic parameters that have been determined.

#### 4. Structural studies of cytochromes $c_3$

X-ray structures of several cytochromes  $c_3$  have been reported and they show that the relative orientations of the haems are highly conserved. However, it is necessary to supplement these data with information from other methods. Apart from obvious problems such as the misplacement of haems in the early X-ray structure of the protein from *Desulfovibrio baculatus* [16], there are uncertainties at the level of conformational difference that may be functionally relevant. The two molecules in the unit cell of the protein from *D. vulgaris* Hildenborough have significantly different geometries for the axial His ligands of haem II: analysis of Fermi contact shifts of the haem substituents gives much better agreement with the geometry found in molecule B. Presumably, such differences are at the level of distortions caused by crystal packing. This is worrying because structures of reduced proteins are normally obtained by reducing crystals of the oxidised protein and so redox-related conformational changes may be restricted by unfavourable contacts. NMR has the advantage that structure may

**Table 3**

Reference rates for reduction of individual haems in cytochrome  $c_3$  by dithionite [10,11]. Standard errors are given in parentheses.

$\times 10^8 \text{ M}^{-1} \text{ s}^{-1}$	Haem I	Haem II	Haem III	Haem IV
<i>D. gigas</i>	7.0 (0.4)	0.0 (0.3)	3.9 (0.5)	10.0 (0.4)
<i>D. vulgaris</i> Hildenborough	15.4 (0.6)	62.9 (0.8)	0.8 (0.8)	11.2 (0.8)
<i>D. desulfuricans</i> ATCC27774	13.9 (5.1)	14.7 (4.9)	2.0 (3.0)	9.6 (3.1)
<i>Dsm. norvegicum</i>	5 (11)	97 (7)	5.1 (0.8)	1 (10)
<i>Dsm. baculatum</i>	16 (9)	98 (10)	3.4 (0.6)	0 (6)
<i>D. africanus</i> (type I)	8.2 (4.0)	16.5 (1.1)	1.2 (0.2)	6.4 (4.0)
<i>D. africanus</i> (type II)	8.1 (0.9)	2.9 (2.7)	0.3 (4.9)	45.9 (4.0)

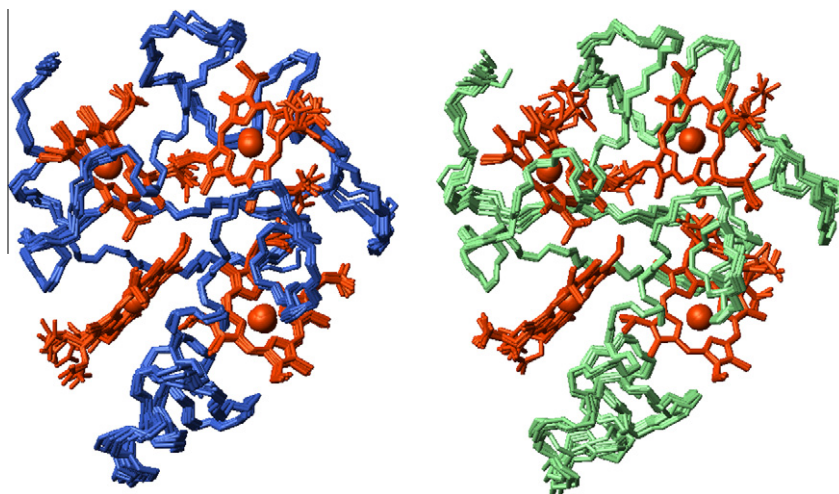


**Fig. 5.** Solution structures of cytochrome  $c_3$  from *D. desulfuricans* ATCC 27774 (left: oxidised, right: reduced). In each case, the polypeptide backbone and haems from the ten structures with the lowest calculated target functions are overlaid [22]. The orientation is similar to that in Fig. 1.

be obtained for oxidised or reduced proteins at a well defined pH, and at ambient temperature. Since the structures may be pH-dependent as well as redox-state-dependent, the thermodynamic properties are needed to set the pH of each sample to have comparable protonation states. The obvious disadvantage of NMR is that the structures are of lower precision than those from X-ray diffraction. This is not the place to go into details of paramagnetic effects and the computational methods that we have developed for structure determination [17,18], but there are some results of interest described below.

We have studied the structures in solution of oxidised and reduced proteins from *Desulfovibrio gigas* [19], *D. vulgaris* [20,21], and *D. desulfuricans* [22]. Many small changes are seen that could contribute to the modulation of the various interactions: in each case, significant motions of the backbone are seen in the 40–70 region with associated movements of several charged groups. The structures of *D. desulfuricans* cytochrome  $c_3$  shown in Fig. 5 show essentially no change in the haem orientations or separations with the exception of a small movement of haem II. Interestingly, this is the haem that is effectively deleted in the homologous trihaem cytochrome from *Desulfuromonas acetoxidans* [23]. The sidechain of Thr24 in the *D. vulgaris* protein and the sequence-aligned Thr28 in that from *D. gigas* (there is no corresponding Thr in *D. desulfuricans* cytochrome  $c_3$ ) rotates, breaking hydrogen bonds that stabilize the oxidised form. Replacing Thr24 with Val in *D. vulgaris* cytochrome  $c_3$  produces small changes in all of the pairwise interactions and makes all of the haem reduction potentials more positive. The redox potential of haem III, which is closest to Thr24, shifts by about 100 mV. At the very least, this is a warning that the position of a single sidechain can affect the properties of the whole protein. In a deeper sense, perhaps we can see why tuning the interactions with residues such as Thr24 is important to the function of the native protein, and this will be discussed in the next section.

It is also important to recognise that the structures of the oxidised and reduced proteins are separated by four electron transfer steps. Although we know, for example, that Thr24 switches its orientation between stage 0 and stage 4, we do not know whether it does so gradually or in a single step and, if so, which.

## 5. Functional studies of cytochromes $c_3$

In short, little has been published so far. Yahata et al. reported “rates of reduction” of a cytochrome  $c_3$  and various mutants by [NiFe] hydrogenase [12]. While it is clear that the kinetic properties are rather more complex, the approximation of a single rate was good enough to demonstrate that changes to the ‘lysine patch’ near to haem IV had a substantial effect.

An obvious deficiency is that cytochromes  $c_3$  from sulphate reducing bacteria are widely believed to transport a pair of protons and a pair of electrons from the periplasmic hydrogenase to a variety of proteins associated with the membrane, but that has never been demonstrated. However, there is a large accumulation of circumstantial evidence and we are close to having direct proof. We note that our assumption requires the cytochromes to cycle between redox stages that are two steps apart, not between the fully oxidised and fully reduced forms (stages 0 and 4). Because the redox-Bohr interactions affect all of the haems, the effect naturally drives the macroscopic reduction potentials (i.e., those averaged across the microstates) together in places (see Fig. 6). For example,  $E_2$  and  $E_3$  are close together near neutral pH in the protein from *D. vulgaris* [7]. That means that the protein is ready to accept two electrons at nearly the same potential and cycle between stages 1 and 3.

The effect can be seen in more detail by using the thermodynamic parameters to calculate the fractional reduction of each

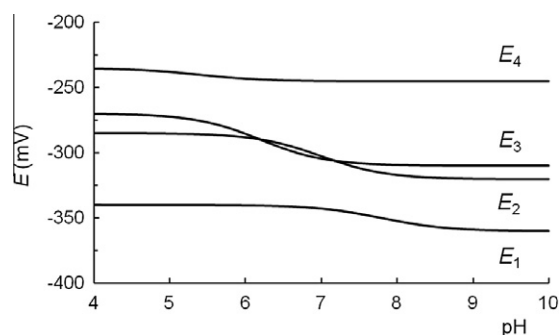


Fig. 6. Macroscopic reduction potentials for the four ET steps in cytochrome  $c_3$  from *D. vulgaris* Hildenborough (after [7]).

haem as a function of solution potential. There is a common tendency for two haems to reduce nearly simultaneously; these are haems I and II in the examples shown in Fig. 7. These are not always the first haems to oxidise, but it may be no coincidence that the paired haems reduce at about  $-300$  mV in each case. This is the region of the redox potentials of the [4Fe–4S] centres in the [NiFe] hydrogenases that transfer electrons to cytochromes  $c_3$ .

The electron acceptor for cytochromes  $c_3$  is understood to be a transmembrane complex denoted Tmc [24]. In *D. vulgaris* and *D.*

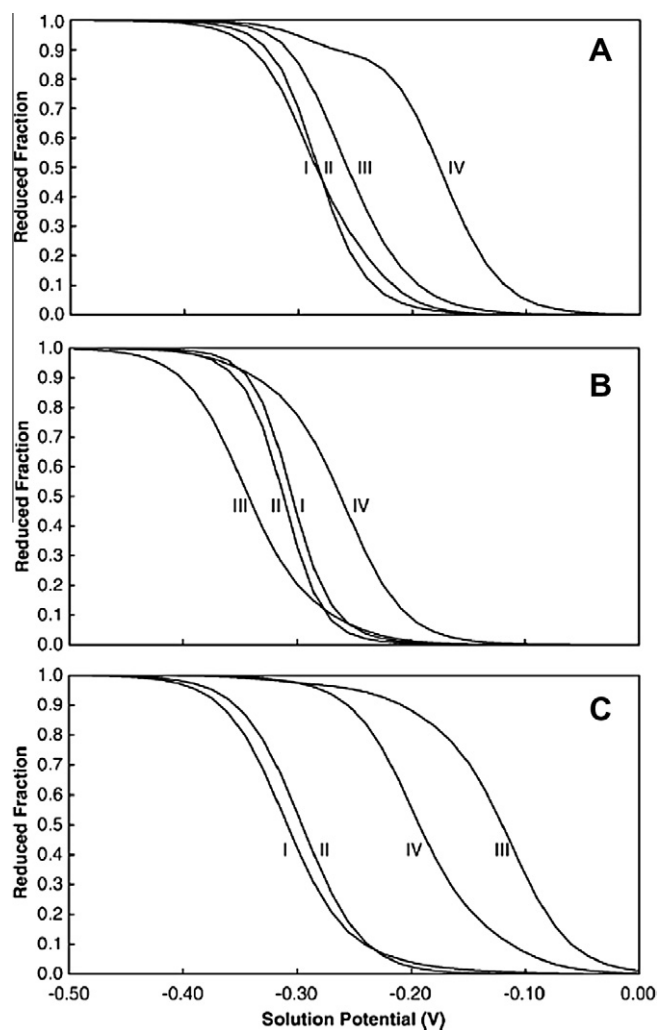
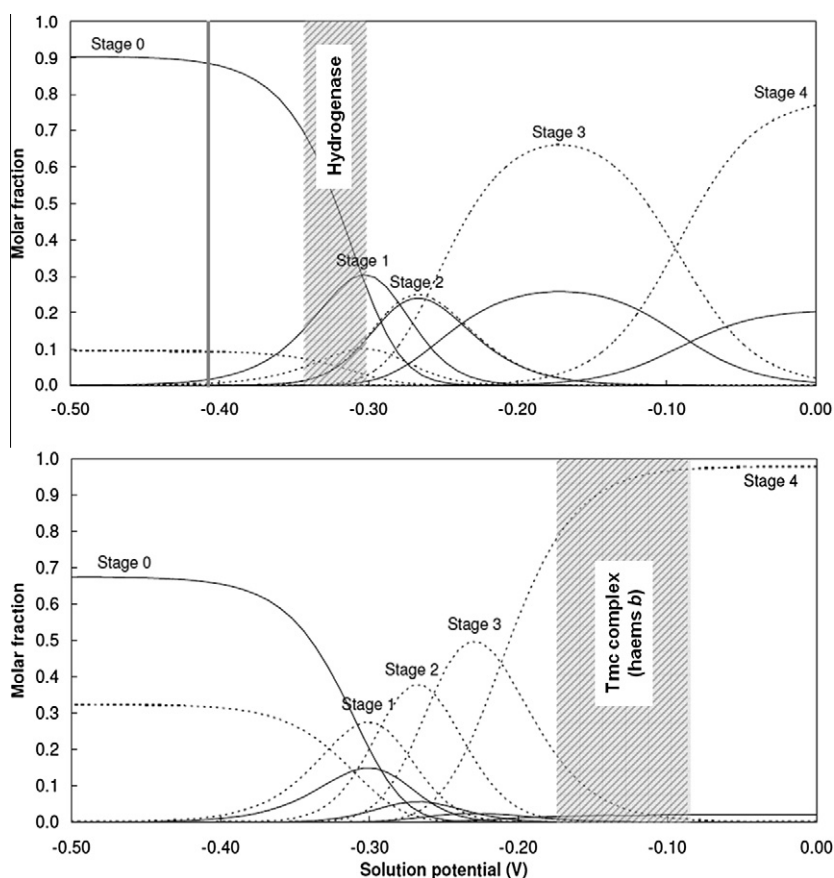


Fig. 7. Calculated fractional reduction of individual haems in cytochromes  $c_3$  from *D. gigas* (A), *D. vulgaris* Hildenborough (B) and *D. desulfuricans* ATCC 27774 (C) at pH 6.5 (after [10]).

*africanus*, the gene coding for this cluster of redox proteins includes a relatively acidic tetrahaem cytochrome  $c_3$  (it lacks the 'lysine patch' near haem IV) that can be obtained in solution [13,25]. This is the "type II" cytochrome  $c_3$  in Tables 1 and 3. They are not easily reduced by [NiFe] hydrogenase except in the presence of type I cytochromes  $c_3$ , which is to be expected if they form the point of contact with the Tmc complex while the type I cytochrome  $c_3$  is the periplasmic electron carrier. The thermodynamic data for the type I and type II cytochromes  $c_3$  from *D. africanus* are shown in Fig. 8, this time by plotting the relative concentrations of each redox stage separated into the protonated and deprotonated components. When the type I cytochrome encounters the Tmc, it should transfer electrons to the type II cytochrome which are then drained by the haems  $b$  in the complex (but note that the protons that are released are not taken up by the type II cytochrome). Hence, when the type I cytochrome separates from the Tmc it is at a potential of around  $-200$  mV and the dominant form is the deprotonated redox stage 3. As it diffuses through the periplasm, the effective potential will not change unless it undergoes further redox reactions. It then encounters the [NiFe] hydrogenase, which presents an effective potential of about  $-300$  mV at the FeS clusters after splitting hydrogen. The major form of the type I cytochrome then becomes protonated stage I, i.e., it picks up two electrons and at least one proton that it will later release to the membrane. The protons need not be transferred directly between the proteins; there is some indication that they may be released to the solvent far from the site of electron transfer [26]. However, transfer via the solvent should not be rate limiting.

The details of the electron transfer from [NiFe] hydrogenase are not clear cut because the equilibrium populations of several stages of the type I cytochrome are significant at about  $-300$  mV, but there are further considerations. First, the reduced hydrogenase has only two electrons available for donation. Secondly, the transient ET complex formed between hydrogenase and type I cytochrome  $c_3$  may modify the properties. Assuming that haem IV is the point of contact, it goes from being partially exposed to the solvent to being effectively buried. Calculations suggest that reduction potentials may be lowered by tens of mV which might leave stage 1 more dominant. On the other hand, rubredoxin, which forms a non-physiological 1:1 complex, has little effect on the redox potentials [9].

The assumption that cytochromes  $c_3$  can diffuse through the periplasm without re-equilibrating deserves comment in view of the surface exposure of all four haems and the non-negligible rate of self-exchange. The rate of these unproductive intermolecular electron transfers may be slow compared with transfers involving the physiological partners, but the single electron transfers that predominate in self-exchange could leave the cytochrome  $c_3$  in an inactive state. This would not be important if the cytochrome  $c_3$  could employ any pair of stages in shuttling electrons but stage 1, for example, could only accept one electron from hydrogenase. The system would avoid blockage if recognition by the partners were redox-state specific. Thus, in the example above, the hydrogenase would only form an encounter complex with cytochrome  $c_3$  in stage 3, and the Tmc would only interact with stage 1. Cytochrome  $c_3$  molecules in other stages resulting from self-exchange



**Fig. 8.** Calculated populations of the five redox stages as a function of solution potential for type I cytochrome  $c_3$  (upper plot) and type II cytochrome  $c_3$  (lower plot) from *D. africanus* at pH 7.2. The population of each stage is separated into the protonated (solid lines) and deprotonated (dashed lines) forms. In the upper plot, a shaded bar indicates the range of reduction potentials of the Fe-S centres of [NiFe] hydrogenase, and the shaded bar in the lower plot indicates the range of the reduction potentials of haems  $b$  in the Tmc complex.

in the periplasm would then have no effect until disproportionation could restore the molecules to active forms.

## 6. Energy transduction by cytochromes $c_3$

The ordering of events in the ET complex is critical to understanding the function of cytochromes  $c_3$ . Electrostatic interactions ought to favour electrons and protons entering the protein together but they probably do not do so simultaneously (such simple Coulomb effects are sometimes referred to as following the principle of electroneutrality, though that strictly applies to atoms or the whole of the solution, not to molecules). Electron transfer is likely to be fast as models show that distances between haems of cytochrome  $c_3$  and redox centres in the donor or acceptor are very short in the ET complex. If there is positive cooperativity between two of the haems then two electrons may be transferred rapidly and consecutively through a single haem at the point of docking; the cytochrome will then have a higher  $pK_a$  and will collect protons. Some hint of the importance of fine tuning the interactions comes from studies of mutants: native proteins tend to have a few dominant microstates, whereas the distribution appears less organised in mutants [27]. Even in the two very similar proteins from *Dsm. norvegicum* and *Dsm. baculatum* which do not display positive cooperativity, a two-electron transfer can still be achieved with the aid of a proton transfer. This is illustrated in the energy level diagram in Fig. 9 calculated at pH 6.15 and solution potential  $-260$  mV using the thermodynamic parameters of the protein from *Dsm. norvegicum* [2]. A deprotonated molecule in stage 3 with haems I, II, and IV oxidised (labelled 124 in Fig. 9) would encounter the donor and receive one electron. In stage 2, the protonated microstate with haems II and IV oxidised (labelled 24) has similar energy to the deprotonated microstate with haems I and II oxidised (labelled 12). Picking up a proton allows a second electron to be transferred, leading to the lowest energy microstate, a protonated form with haem II oxidised.

On encountering the acceptor complex, electrons are released, which lowers the  $pK_a$  and drives out protons. Since the electron flow is effectively dragging protons in its wake, energy is transferred from electrons to protons. The protons enter the protein with a high  $pK_a$  and leave it when the protein  $pK_a$  is lower. This is illustrated clearly by the macroscopic  $pK_a$ s calculated for the cytochrome  $c_3$  from *D. vulgaris*: a two-electron transfer takes the protein from redox stage 3 to stage 1, then the redox-Bohr group has a  $pK_a$  of 7.23 (see Table 4) and receives a proton. After diffusion through the periplasm, electrons are transferred to the membrane complex and the  $pK_a$  drops to 5.58, enabling the release of protons to a more acidic medium.

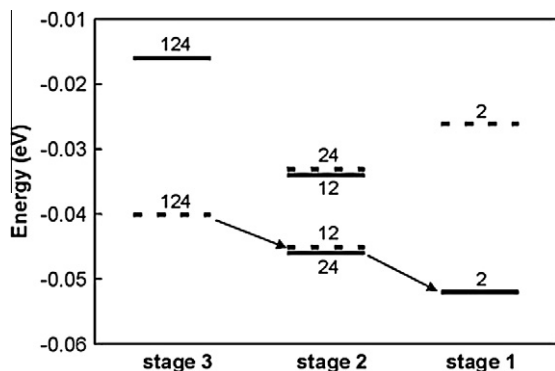


**Fig. 9.** Energies of the most stable microstates in of cytochrome  $c_3$  from *Dsm. norvegicum* at pH 6.15 and solution potential  $-260$  mV. A deprotonated (dashed lines) microstate in stage 3 may collect an electron, then a proton, then a second electron to give a protonated (solid lines) microstate in stage 1 (from [2]).

**Table 4**

Macroscopic  $pK_a$ s in the five redox stages of cytochrome  $c_3$  from *D. vulgaris* Hildenborough [10].

Stage 0	Stage 1	Stage 2	Stage 3	Stage 4
7.68	7.23	6.47	5.58	5.19

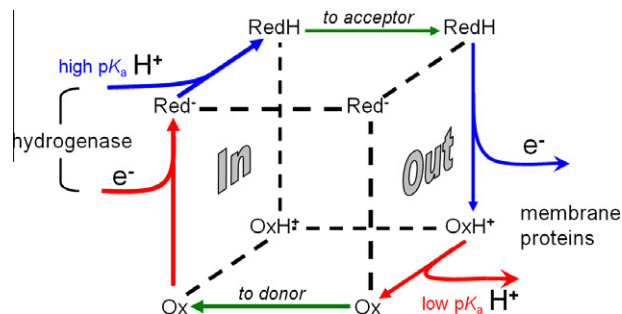


**Fig. 10.** A 'cubane' diagram illustrating energy transduction by cytochromes  $c_3$ . The cytochrome receives electrons followed by protons from the donor hydrogenase. It then diffuses through the periplasm to the membrane where it delivers electrons followed by protons. The redox-Bohr interaction ensures that electrons are delivered with the protein having a higher reduction potential than when they were received and protons are delivered from groups with a lower  $pK_a$  than when they were received, i.e., the electrons lose energy and the protons gain it.

The importance of the ordering of individual events is shown clearly in the 'cubane' diagram favoured by António Xavier that is shown in Fig. 10. Solid lines represent the electron and proton transfer and diffusion steps undertaken by the type I cytochrome  $c_3$ . The dashed lines all represent unproductive transitions.

## 7. New directions

Because of its ability to distinguish individual haems, NMR is the method of choice for studying moderately fast electron transfer reactions in haem proteins. By contrast, a stopped flow experiment that reacted reduced type I cytochrome  $c_3$  with oxidised type II cytochrome would see virtually nothing happen because the total oxidised haem would not change. NMR is actually too slow to follow ET reactions in that way, but it does have the remarkable capability of monitoring electron exchange between haems in mixtures at equilibrium. Thus the mixing time dependence of the cross-peak intensities in 2D exchange experiments such as those shown in Fig. 3 can reveal the number of electrons transferred in each encounter. The results of experiments to measure electron transfer rates in mixtures of type I and type II cytochrome  $c_3$ , which are physiological ET partners, will be reported elsewhere. Similar experiments with hydrogenase are a little more difficult because of the tendency for it to be poisoned by oxygen, which it is commonly used to adjust solution potentials in the NMR tube.

The insights gained from these studies have also inspired other models. In 2002, António Xavier proposed an elegant and original model for the mechanism of proton pumping in cytochrome  $c$  oxidase [28,29]. His model was based on published data for this enzyme and the observation of both positive and negative cooperativities in cytochromes  $c_3$  and cytochrome  $c'$  [30,31], and also on the well-known conformational transitions in haemoglobin. The model is novel insofar as it is based on anti-electrostatic cooperativities involving haem  $a$  and a nearby protonatable group located on the P side of the haem. The pH dependence of the reduction potential of haem  $a$  does not agree with the usual 60 mV per pH unit: Xavier simulated this behaviour with a sum of two acid/base groups interacting with haem  $a$ . One of these groups displays

the usual positive redox–Bohr ( $rB^+$ ) effect corresponding to an electrostatic interaction and the other displays a negative redox–Bohr ( $rB^-$ ) effect, which is anti-electrostatic since the entrance of an electron provokes the ejection of a proton. According to the model, the proton pump is centred on the  $rB^-$  group. The pumping cycle would begin with the  $rB^-$  group protonated and haem *a* oxidised. Upon reduction of haem *a*, the protein would undergo a structural change that causes a decrease in the  $pK_a$  of the  $rB^-$  group, which results in proton ejection to the P side. The model is phenomenologically similar to the mechanism of proton pumping by bacteriorhodopsin [32] in which the proton is already in place at the onset of the light cycle and the photon brings about a conformational change that ejects the proton to the correct side of the membrane. The elegance of the model also resides in the fact that energy transduction would be linked to a charge separation event, as it is the case in the light reactions of photosynthesis. In fact, contrary to ‘electroneutrality’, charge separation leads to a situation where the system can perform work. The model was criticised and forgotten because it relies on a conformational change and there is no evidence for a significant alteration of the structure during the redox cycle of cytochrome *c* oxidase [33]. However, as Xavier pointed out, small localised conformational changes can be functionally relevant, as observed with the tetrahaem cytochromes  $c_3$  [28,29]. In fact, more recent models invoke similar conformational changes to achieve gating of the pump [34].

The original minimum model was expanded in 2004 to include the role of the  $rB^+$  group [29]. This acid/base group would be protonated upon reduction of haem *a* and, as soon as the electron moves from this haem to the binuclear centre, the proton would be transferred to the catalytic site where it would be used in the reduction of oxygen to water. Although purely conceptual because the two  $rB$  groups were not identified, this model could explain some experimental results such as the pumping of protons at the onset of the reductive phase of the catalytic cycle or the pulsed/resting switch of the protein. Moreover, it predicted that a change in the  $pK_a$  of the  $rB^-$  group, would result in a protein that would be able to perform normal catalysis but would not pump protons because the  $rB^-$  group would be either always protonated ( $pK_a$  higher than wild type) or always deprotonated ( $pK_a$  lower than wild type), as in the mutants recently described in the literature [35,36]. Perhaps it is time to reconsider the involvement of anti-electrostatic electron–proton interactions in the proton pumping mechanism of cytochrome *c* oxidase.

## Acknowledgements

This work was supported by Centro de Ressonância Magnética António Xavier (CERMAX) with funding from REDE/1517/RMN/2005 and PTDC/QUI/65640/2006, both from Fundação para a Ciência e a Tecnologia, Portugal.

## References

- [1] Louro, R.O. (2007) Proton thrusters: overview of the structural and functional features of soluble tetrahaem cytochromes  $c(3)$ . *J. Biol. Inorg. Chem.* 12, 1–10.
- [2] Correia, I.J. et al. (2004) Proton-assisted two-electron transfer in natural variants of tetrahaem cytochromes from *Desulfomicrobium* sp.. *J. Biol. Chem.* 279, 52227–52237.
- [3] Dobson, C.M., Hoyle, N.J., Gerald, C.F., Bruschi, M., Legall, J., Wright, P.E. and Williams, R.J.P. (1974) Outline structure of cytochrome  $c_3$  and consideration of its properties. *Nature* 249, 425–429.
- [4] Dervartanian, D.V., Xavier, A.V. and Legall, J. (1978) EPR determination of oxidation–reduction potentials of hemes in cytochrome  $c_3$  from *Desulfovibrio vulgaris*. *Biochimie* 60, 321–325.
- [5] Santos, H., Moura, J.J.G., Moura, I., Legall, J. and Xavier, A.V. (1984) NMR studies of electron-transfer mechanisms in a protein with interacting redox centers – *Desulfovibrio gigas* cytochrome  $c_3$ . *Eur. J. Biochem.* 141, 283–296.
- [6] Louro, R.O., Catarino, T., LeGall, J., Turner, D.L. and Xavier, A.V. (2001) Cooperativity between electrons and protons in a monomeric cytochrome  $c_3$ : the importance of mechano-chemical coupling for energy transduction. *ChemBioChem* 2, 831–837.
- [7] Turner, D.L., Salgueiro, C.A., Catarino, T., Legall, J. and Xavier, A.V. (1996) NMR studies of cooperativity in the tetrahaem cytochrome  $c(3)$  from *Desulfovibrio vulgaris*. *Eur. J. Biochem.* 241, 723–731.
- [8] Pessanha, M. et al. (2009) Tuning of functional heme reduction potentials in *Shewanella fumarate reductases*. *Biochim. Biophys. Acta: Bioenerg.* 1787, 113–120.
- [9] Salgueiro, C.A., Morgado, L., Fonseca, B., Lamosa, P., Catarino, T., Turner, D.L. and Louro, R.O. (2005) Binding of ligands originates small perturbations on the microscopic thermodynamic properties of a multicentre redox protein. *FEBS J.* 272, 2251–2260.
- [10] Paquete, C.M., Turner, D.L., Louro, R.O., Xavier, A.V. and Catarino, T. (2007) Thermodynamic and kinetic characterisation of individual haems in multicentre cytochromes  $c(3)$ . *Biochim. Biophys. Acta: Bioenerg.* 1767, 1169–1179.
- [11] Paquete, C.M., Pereira, P.M., Catarino, T., Turner, D.L., Louro, R.O. and Xavier, A.V. (2007) Functional properties of type I and type II cytochromes  $c(3)$  from *Desulfovibrio africanus*. *Biochim. Biophys. Acta: Bioenerg.* 1767, 178–188.
- [12] Yahata, N., Saitoh, T., Takayama, Y., Ozawa, K., Ogata, H., Higuchi, Y. and Akutsu, H. (2006) Redox interaction of cytochrome  $c(3)$  with [NiFe] hydrogenase from *Desulfovibrio vulgaris* Miyazaki F. *Biochemistry* 45, 1653–1662.
- [13] Pieuille, L., Morelli, X., Gallice, P., Lojou, E., Barbier, P., Czjzek, M., Bianco, P., Guerlesquin, F. and Hatchikian, E.C. (2005) The type I/type II cytochrome  $c(3)$  complex: an electron transfer link in the hydrogen-sulfate reduction pathway. *Journal of Molecular Biology* 354, 73–90.
- [14] Louro, R.O., Catarino, T., Paquete, C.M. and Turner, D.L. (2004) Distance dependence of interactions between charged centres in proteins with common structural features. *FEBS Lett.* 576, 77–80.
- [15] Catarino, T. and Turner, D.L. (2001) Thermodynamic control of electron transfer rates in multicentre redox proteins. *ChemBioChem* 2, 416–424.
- [16] Coutinho, I.B., Turner, D.L., Legall, J. and Xavier, A.V. (1992) Revision of the heme-core architecture in the tetrahaem cytochrome  $c_3$  from *Desulfovibrio baculatus* by 2-dimensional  $^1H$  NMR. *Eur. J. Biochem.* 209, 329–333.
- [17] Turner, D.L., Salgueiro, C.A., Schenkels, P., Legall, J. and Xavier, A.V. (1995)  $^{13}C$  NMR studies of the influence of axial ligand orientation on heme electronic structure. *Biochim. Biophys. Acta: Protein Struct. Mol. Enzymol.* 1246, 24–28.
- [18] Turner, D.L., Brennan, L., Chamberlin, S.G., Louro, R.O. and Xavier, A.V. (1998) Determination of solution structures of paramagnetic proteins by NMR. *Eur. Biophys. J. Biophys. Lett.* 27, 367–375.
- [19] Brennan, L., Turner, D.L., Messias, A.C., Teodoro, M.L., LeGall, J., Santos, H. and Xavier, A.V. (2000) Structural basis for the network of functional cooperativities in cytochrome  $c(3)$  from *Desulfovibrio gigas*: solution structures of the oxidised and reduced states. *J. Mol. Biol.* 298, 61–82.
- [20] Messias, A.C., Aguiar, A.P., Brennan, L., Salgueiro, C.A., Saraiva, L.M., Xavier, A.V. and Turner, D.L. (2006) Solution structures of tetrahaem ferricytochrome  $c(3)$  from *Desulfovibrio vulgaris* (Hildenborough) and its K45Q mutant: the molecular basis of cooperativity. *Biochim. Biophys. Acta: Bioenerg.* 1757, 143–153.
- [21] Messias, A.C., Kastrau, D.H.W., Costa, H.S., LeGall, J., Turner, D.L., Santos, H. and Xavier, A.V. (1998) Solution structure of *Desulfovibrio vulgaris* (Hildenborough) ferrocyclochrome  $c(3)$ : structural basis for functional cooperativity. *J. Mol. Biol.* 281, 719–739.
- [22] Paixao, V.B., Vis, H. and Turner, D.L. (2010) Redox linked conformational changes in cytochrome  $c(3)$  from *Desulfovibrio desulfuricans* ATCC 27774. *Biochemistry* 49, 9620–9629.
- [23] Coutinho, I.B., Turner, D.L., Liu, M.Y., LeGall, J. and Xavier, A.V. (1996) Structure of the three-haem core of cytochrome  $c-551.5$  determined by  $^1H$  NMR. *J. Biol. Inorg. Chem.* 1, 305–311.
- [24] Pereira, P.M., Teixeira, M., Xavier, A.V., Louro, R.O. and Pereira, I.A.C. (2006) The Tmc complex from *Desulfovibrio vulgaris* Hildenborough is involved in transmembrane electron transfer from periplasmic hydrogen oxidation. *Biochemistry* 45, 10359–10367.
- [25] Valente, F.M.A., Saraiva, L.M., LeGall, J., Xavier, A.V., Teixeira, M. and Pereira, I.A.C. (2001) A membrane-bound cytochrome  $c(3)$ : a type II cytochrome  $c(3)$  from *Desulfovibrio vulgaris* Hildenborough. *ChemBioChem* 2, 895–905.
- [26] Teixeira, V.H., Soares, C.M. and Baptista, A.M. (2008) Proton pathways in a [NiFe]-hydrogenase: a theoretical study. *Proteins: Struct. Funct. Bioinform.* 70, 1010–1022.
- [27] Salgueiro, C.A., da Costa, P.N., Turner, D.L., Messias, A.C., van Dongen, W., Saraiva, L.M. and Xavier, A.V. (2001) *Desulfovibrio vulgaris* (Hildenborough) cytochrome  $c(3)$  probed by site-specific mutagenesis. *Biochemistry* 40, 9709–9716.
- [28] Xavier, A.V. (2002) A mechano-chemical model for energy transduction in cytochrome *c* oxidase: the work of a Maxwell’s god. *FEBS Lett.* 532, 261–266.
- [29] Xavier, A.V. (2004) Thermodynamic and choreographic constraints for energy transduction by cytochrome *c* oxidase. *Biochim. Biophys. Acta: Bioenerg.* 1658, 23–30.
- [30] Costa, H.S., Santos, H., Turner, D.L. and Xavier, A.V. (1992) Involvement of a labile axial histidine in coupling electron and proton transfer in *Methylophilus methylotrophus* cytochrome  $c'$ . *Eur. J. Biochem.* 208, 427–433.

- [31] Enguita, F.J., Pohl, E., Turner, D.L., Santos, H. and Carrondo, M.A. (2006) Structural evidence for a proton transfer pathway coupled with haem reduction of cytochrome *c*' from *Methylophilus methylotrophus*. *J. Biol. Inorg. Chem.* 11, 189–196.
- [32] Luecke, H., Schobert, B., Richter, H.T., Cartailler, J.P. and Lanyi, J.K. (1999) Structural changes in bacteriorhodopsin during ion transport at 2 Angstrom resolution. *Science* 286, 255–260.
- [33] Wikstrom, M. (2004) Cytochrome *c* oxidase: 25 years of the elusive proton pump. *Biochim. Biophys. Acta: Bioenerg.* 1655, 241–247.
- [34] Kim, Y.C., Wikstrom, M. and Hummer, G. (2009) Kinetic gating of the proton pump in cytochrome *c* oxidase. *Proc. Natl. Acad. Sci. USA* 106, 13707–13712.
- [35] Lee, H.J., Svahn, E., Swanson, J.M.J., Lepp, H., Voth, G.A., Brzezinski, P. and Gennis, R.B. (2010) Intricate role of water in proton transport through cytochrome *c* oxidase. *J. Am. Chem. Soc.* 132, 16225–16239.
- [36] Chakrabarty, S., Namslauer, I., Brzezinski, P. and Warshel, A. (2011) Exploration of the cytochrome *c* oxidase pathway puzzle and examination of the origin of elusive mutational effects. *Biochim. Biophys. Acta: Bioenerg.* 1807, 413–426.